# In situ monitoring and optimization of CuAAC-mediated protein functionalization of biosurfaces

Peer-reviewed author version

VRANKEN, Tom; STEEN REDEKER, Erik; Miszta, Adam; BILLEN, Brecht; Hermens, Wim; de Laat, Bas; ADRIAENSENS, Peter; GUEDENS, Wanda & CLEIJ, Thomas (2017) In situ monitoring and optimization of CuAAC-mediated protein functionalization of biosurfaces. In: SENSORS AND ACTUATORS B-CHEMICAL, 238, p. 992-1000.

DOI: 10.1016/j.snb.2016.07.071
Handle: http://hdl.handle.net/1942/23226

# In situ monitoring and optimization of CuAAC-mediated protein functionalization of biosurfaces

*Tom Vranken*[a], *Erik Steen Redeker*[a,b,*], *Adam Miszta*[c,d], *Brecht Billen*[a], *Wim Hermens*[c], *Bas de Laat*[c,d], *Peter Adriaensens*[a], *Wanda Guedens*[a] *and Thomas J. Cleij*[a,b]

[a] Organic and Bio-Polymer Chemistry, Institute for Materials Research, Hasselt University, Diepenbeek, BE 3590, Belgium

[b] Maastricht Science Programme, Maastricht University, Maastricht, 6200 MD, The Netherlands.

[c] Synapse B.V., Maastricht, 6229 EV, The Netherlands

[d] Cardiovascular Research Institute Maastricht, Maastricht, 6229 ER, The Netherlands

*Corresponding Author: erik.steenredeker@maastrichtuniversity.nl

**Abstract**

With the current trend to miniaturize bioactive surfaces to micro- or nanometer scale, the strategy of immobilization becomes more important. Therefore, there is a growing need for protein immobilization techniques that create both stable and homogeneously covered surfaces in a reproducible way. One of the most promising methods to achieve this is the combination of biological receptors with 'click' chemistry, like the Copper catalyzed Alkyne Azide Cycloaddition (CuAAC). This work presents a full optimization of all aspects of the 'click' chemistry reaction between proteins and surfaces in order to create covalently and homogeneously covered biosurfaces. The coupling procedure is monitored by *in situ* ellipsometry, a unique characterization technique that offers the opportunity to quantify minute amounts of surface coupled protein mass in real-time. The optimization involves the azidification of a solid silicon support, the alkynation of two proteins, *Staphylococcus aureus* Protein A (SpA) and Maltose Binding Protein (MBP), as well as the development of a highly reproducible CuAAC 'click' coupling protocol. Using the here optimized protocol, active and reproducible biolayers can be created rapidly. The proposed surface biofunctionalization method combined with ellipsometry forms a unique and promising platform towards the development of highly sensitive, accurate biosensors.

**Keywords**

Protein surface functionalization, Bio-orthogonal chemistry, CuAAC 'Click' chemistry, Ellipsometry, *Staphylococcus aureus* Protein A, Maltose Binding Protein.

## 1. Introduction

During the last decade several exciting examples of innovative microarrays and biosensing applications have been developed [1-6]. Typical sensing devices consist of three main parts, *i.e*. the sensing target receptor, the transducer surface and the readout system. The current trend of miniaturizing these devices is one of the key challenges in the field of advanced biosensing, since downscaled biosensors can facilitate multiple parallel measurements, with smaller amounts of expensive biological receptor material. Nowadays, a wide variety of target receptors is described in literature, *e.g*. DNA, phospholipids, glycosaminoglycans, enzymes, antibodies, cells and molecularly imprinted polymers (MIPs) [7-14]. Especially the quest for durable coupling methods to attach proteins to surfaces is of considerable interest in biomedical, biochemical and immunological research [15-18]. For miniaturized protein-based devices, an optimal and uniform coverage of the transducer surface with proteins becomes even more crucial. The coupling reaction of choice must be highly efficient, selective, reproducible, non-destructive, without side reactions and, if possible, rapid.

Many different strategies, such as physical adsorption, affinity-based interactions and covalent couplings have been reported to immobilize proteins to the transducer surfaces [19-21]. Coupling methods based on weak interactions (hydrogen bonds, electrostatic, hydrophobic and van der Waals interactions) can result in oriented immobilization but are reversible in nature, possibly leading to stability and reproducibility problems. On the other

hand, covalent coupling could be formed using the naturally present amino acid chemistry such as, for example, amines in lysines or thiols in cysteines. Although this leads to stable coverage, there is generally no control over the orientation of the protein on the surface due to the presence of multiple copies of the same amino acids [22,23]. In either case, these methods often lead to sub-optimal sensitivity of the biosensing devices, due to lack of uniform biomolecule orientation, stability and/or reproducibility [24,25]. It is therefore important to develop methods that direct both orientation *and* stability.

One of the most promising methods for covalent protein immobilization is based on 'click' chemistry, *e.g.* the copper(I) catalyzed 1,3-dipolar cycloaddition of azides and alkynes (CuAAC) [21,26]. The CuAAC reaction is well known for its high specificity and efficiency, bioorthogonal properties (i.e. azides and alkynes do not interfere with native biochemical processes [27]) and lack of side reactions [28,29]. Furthermore, the coupling reaction can be accomplished in aqueous solution under mild physiological conditions and on a variety of biomolecules and transducer supports [30-34].

CuAAC has been extensively used for the conjugation, immobilization, and purification of several biomolecules: DNA, peptides, proteins, oligosaccharides and glycoconjugates have been labelled with various attachements [35,36]. With regard to the labeling in living organisms, however, CuAAC suffers from the cytotoxicity of Cu(I) and has therefore mainly been applied to labeling reactions in the extracellular space [37]. Since the proven biological applicability and the fact that both azide and alkyne groups can be appended to biomolecules without altering their function or metabolic processing, reactions between alkynes and azides have been adapted to reduce the cell toxicity [38]. One approach to do this is by removing the Cu(I) requirement in the reaction. By using cyclooctynes, for example, the reaction is activated by ring strain in the so-called 'Strain-promoted azide-alkyne cycloaddition' or SPAAC [39]. However, the relatively large size and hydrophobic nature of the cyclooctyne

components can affect the biological properties of the biomolecule to which it is attached [40]. Copper-free SPAAC reactions are also 10-100 times slower than classical CuAAC reaction [35,40]. In addition, strained cyclooctyne synthesis is difficult compared to terminal alkynes and although available, commercial SPAAC components are still expensive. A second approach to improve the biocompatibility of CuAAC is the use of ligands for Cu(I) such as tris-(benzyltriazolylmethyl)amine (TBTA) [41] and tris(3-hydroxypropyltriazolylmethyl)amine (THPTA) [42]. These ligands serve multiple purposes; they not only accelerate the cycloaddition reaction, they also act as sacrificial reductants protecting the copper from oxidation and help to protect cells and biomolecules [38,43]. TBTA and the water-soluble THPTA are both used in the present study.

A secondary advantage of the use of Cu(I) as a catalyst in the present study is that it acts as a 'on-off' switch, making it possible to see a difference between immobilization through a click reaction reaction or by physical adsorption by respectively presence or absence of Cu(I) in the reaction. However, protein functionalized surfaces created with 'click' chemistry often still suffer from reproducibility issues and insufficient and/or non-homogeneous protein coverage.

This work therefore presents a full optimization of all aspects of the 'click' chemistry reaction between proteins and surfaces. This is exemplified by the 'click' mediated immobilization of two model proteins, Protein A (SpA, a 42 kDa immunoglobulin-binding surface protein of *Staphylococcus aureus*) and Maltose Binding Protein (MBP, a 42 kDa soluble periplasmic protein [44]). For this, SpA and MBP are both modified with an alkyne linker *via* their endogenous surface lysines. Lysines are present in most proteins, and can make up to over 10% of the overall amino acid sequence and are frequently located on the surface of the protein [45]. However this method does not lead to single and site-specific protein modification, for the purpose of this study, i.e. optimization of the 'click' mediated

protein immobilization, lysines offer a relatively easy method to add bio-orthogonal chemistry to proteins. Conjugation with the amine group of lysine is very often done with N-Hydroxysuccinimide (NHS) esters resulting in the formation of stable peptide bonds. In the present study an alkyne-containing NHS-ester is used to alkynate SpA and MBP. The alkyne-modified proteins are subsequently immobilized using CuAAC onto silica slides that are treated with the complementary reactive azides.

During the optimization of the reaction conditions, the binding efficiency was evaluated using *in situ* ellipsometry. This technique is a non-destructive, optical technique based on changes in the orientation of two polarizer prisms [46] and gives us a unique opportunity to evaluate the CuAAC reaction in real-time with nanogram accuracy. To our knowledge the real-time assessment of CuAAC-immobilized protein layers has never been performed before. Ellipsometry offers the opportunity to not only detect and quantify the formed protein layer, but also to observe the adsorption towards the surface while it happens. The target-binding efficiency of this method is compared to commonly used immobilization techniques, *i.e.* physical adsorption and EDC/NHS coupling using a direct reaction between the lysines and carboxylated slides.

For obvious reasons, it is also important that the alkynation, the number of modifications on the protein and the immobilization process do not induce conformational changes or influence or block the active site(s) of the protein. Therefore, the activity of SpA and MBP after immobilization has been assessed using binding studies with human IgG (binding the Fc domain) and monoclonal anti-MBP (Fab domain), respectively. Again ellipsometry was used to quantify the amount of surface coupled antibody.

## 2. Materials and Methods

### 2.1. Materials

Zeba micro spin desalting columns (7K MWCO, 0.5 mL), SpA (Cowan strain, recombinant, *Staphylococcus aureus subsp. aureus* strain NCTC 8325, expressed in *E. coli*) and human IgG (hIgG) were obtained from Thermo Scientific. Carboxylated, hydrophilic silicon slides, PVC coated slides and 'washing buffer' (WB) were developed by Synapse B.V., Maastricht, The Netherlands. 1-ethyl-3-(3-dimethylaminopropyl) carbodiimide (EDC), *N*-hydroxysuccinimide (NHS), bromopropylamine hydrobromide and sodium azide were purchased from Acros. Tris[(1-benzyl-1H-1,2,3-triazol-4-yl)methyl] amine (TBTA), tris(3-hydroxypropyltriazolylmethyl)amine (THPTA), diethylene glycolamine, sodium L-ascorbate (NaAsc), 4-(2-hydroxyethyl)-1-piperazineethanesulfonic acid (HEPES), monoclonal Anti-Maltose Binding Protein antibody (anti-MBP, clone-17), 2-(*N*-morpholino)ethanesulfonic acid (MES), sodium acetate trihydrate and 5-hexynoic acid tris(2-carboxyethyl)phosphine (TCEP) were obtained from Sigma-Aldrich. MBP was obtained from the pMXB10 vector purchased from New England Biolabs.

### 2.2. Solutions

220 mM HEPES buffer pH 6.8; 10 mM alkyne NHS in acetonitrile; 1 M diethylene glycolamine pH 7.5; PBS buffer pH 7.4: 137 mM NaCl, 27 mM KCl, 10 mM $Na_2HPO_4$, 2 mM $KH_2PO_4$; 0.1 M glycine-0.2 M NaCl pH 2.5; 0.01 M sodium acetate buffer pH 4; 0.5% SDS in $H_2O$; 0.01 M MES buffer pH 4; 0.05 M Tris-0.1 M NaCl buffer pH 7.5. Buffers were prepared with Milli-Q water.

### 2.3. Instruments

147 Contact angle measurements were performed with a dataphysics OCA 15+ goniometer
148 (Filderstadt, Germany). Contour ellipse fitting of the water droplets was done by the SCA 1.0
149 software. The droplet size was 1 $\mu$L dispensed at 0.1 $\mu$L/s.

150 Ellipsometry was performed on an ellipsometer with eight cuvettes equipped with
151 magnetic stirrers, monitoring time-dependent changes in polarizer angle, analyzer angle and
152 reflected light intensity [46]. A reference surface mass was recorded for each slide before the
153 start of the binding monitoring.

154 2.4. Azidification of the carboxylated silicon slides

155 The azide linker, 3-azido-1-aminopropane (AAP, **(1)** in figure 1), synthesized as described
156 by Hatzakis [47], was attached to the carboxylated silicon slides using EDC/NHS chemistry.
157 The slides were immersed into a mixture of EDC (0.2 M), NHS (0.045 M) and AAP (0.23 M)
158 in HEPES buffer for 3 hours. Remaining NHS esters on the surface of the slides were
159 neutralized with diethylene glycolamine for 45 min after which the slides were rinsed with
160 Milli-Q water and dried with nitrogen. The water droplet contact angles on the slides were
161 measured and compared to the contact angles on carboxylated slides before azidification. A
162 change in contact angle is an indication for the change in hydrophilicity of the surface caused
163 by the change of the chemical groups (carboxylic acid to azides) on the surface.

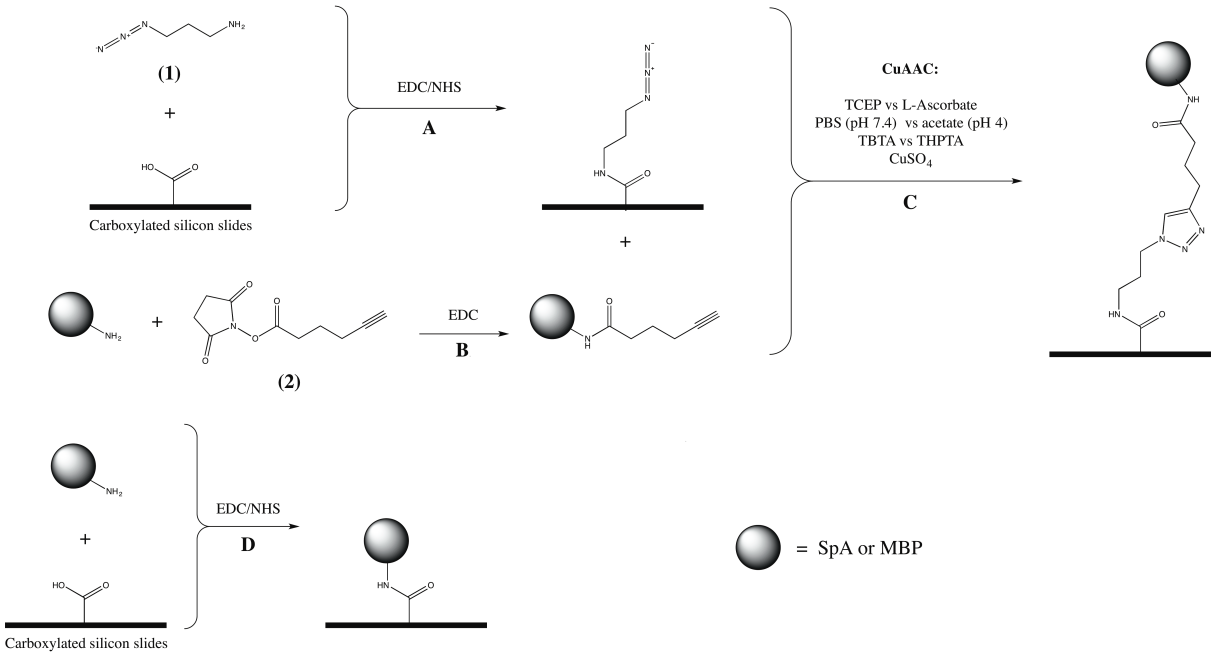


164

165 **Figure 1.** Reaction schemes of the azidification of the silicon slides (A),
166 alkynation of proteins (B), CuAAC immobilization of the proteins (C) and
167 EDC/NHS mediated immobilization of proteins (D).

168

169 2.5. Alkynation of SpA and MBP

170 SpA and MBP were alkynated by the reaction of an NHS linker with lysine. The alkyne
171 NHS ester, 2,5-dioxopyrrolidin-1-yl-hex-5-ynoate ((**2**) in figure 1), was synthesized according
172 to Jagadish [48].

173 The proteins were alkynated by adding the alkyne NHS ester to an SpA solution of 17.7
174 $\mu$M in PBS and an MBP solution of 3.5 $\mu$M in PBS, yielding alkyne-SpA (A-SpA) and
175 alkyne-MBP (A-MBP) respectively. Appropriate NHS ester concentrations were added to
176 both proteins leading to a theoretical functionalization level of 16% of the present lysines (63
177 for SpA [49,50] and 36 for MBP [51]). In addition, a theoretically fully (100%) alkynated
178 SpA (fA-SpA) and MBP (fA-MBP) were obtained by adding a 1.5 molar excess (to the total

number of lysines) of the alkyne NHS ester. After 3 hours the reaction mixture was filtered using a Zeba micro spin desalting column. Chemical modification by alkynation was demonstrated by native PAGE, visualizing the changes in electrophoretic mobility caused by the alterations in the overall charge of the proteins.

### 2.6. CuAAC immobilization of A-SpA

A screening of optimal 'click' reaction conditions was performed by using different combinations of reducing agents (TCEP *versus* sodium L-ascorbate), buffers (PBS pH 7.4 v*ersus* sodium acetate buffer pH 4) and ligands, i.e. the commonly used non-polar TBTA or the water-soluble THPTA. Since TBTA is not soluble in water, DMSO is added to the reaction mixtures containing TBTA. The amount of immobilized SpA in the different reaction conditions was measured as the average surface mass (ASM). All mixtures contained 1 $\mu$M A-SpA and 0.5 mM $CuSO_4$. 64 Azidified slides were placed in the 8 different reaction mixtures for 18 hours at room temperature without stirring, resulting in 8 samples for each immobilization condition. After the reactions, the ASM was determined by ellipsometry analysis. The different reaction conditions are given in Table 1.

**Table 1.** Reaction mixtures used for the immobilization of SpA in either sodium acetate buffer pH 4 or PBS pH 7.4. All mixtures contain 1$\mu$M of protein.

| Mixture | Reducing agent (mM) | | Ligand (mM) | | Cu Catalyst (mM) | |
|---|---|---|---|---|---|---|
| **1** | **NaAsc.** | 2.50 | **THPTA** | 1.00 | $CuSO_4$ | 0.50 |
| **2** * | **TCEP** | 0.85 | **TBTA** | 1.00 | $CuSO_4$ | 0.50 |
| **3** | **TCEP** | 0.85 | **THPTA** | 1.00 | $CuSO_4$ | 0.50 |
| **4** * | **NaAsc.** | 2.50 | **TBTA** | 1.00 | $CuSO_4$ | 0.50 |

*contains 2.5 % DMSO.

198 Additional to the coupling reaction of A-SpA to the azidified slides, three control
199 experiments were simultaneously performed: 1) reaction between azidified slides and
200 wildtype SpA, 2) carboxylated slides and A-SpA and 3) carboxylated slides and wildtype
201 SpA. Reaction time and concentrations of the other reactants were left unchanged.

202 Washing of the samples after immobilization was performed in three subsequent steps
203 using different buffers: PBS to remove the protein solution containing the reagents and the
204 excess of protein on the surface, Washing Buffer to interrupt the electrostatic interactions and
205 finally SDS to remove hydrophobic bonds.

206 To follow the 'click' reaction in real-time and to determine the rate of immobilization, the
207 ASM of A-SpA using *Mixture 1* in acetate buffer and *Mixture 2* in PBS was monitored after 0
208 s, 1800 s (0.5h) and 65000 s (18h).

209 To determine the influence of the protein concentration on the CuAAC coupling, five
210 additional A-SpA solutions were tested, *i.e.* 0.034 $\mu$M, 0.068 $\mu$M, 0.102 $\mu$M, 0.136 $\mu$M and
211 0.500 $\mu$M. The immobilization was performed in *Mixture 1* in acetate buffer *in duplo* for
212 every protein concentration for 30 minutes. The ASM after coupling as well as after the
213 washing steps was determined by ellipsometry.

214 To test the effect of the reaction volume on the immobilization efficiency, immobilization
215 was performed *via* a drop method. For this, eight azide functionalized slides were put
216 horizontally in a water vapor saturated environment at room temperature. Subsequently one
217 drop (30 $\mu$L), containing 1 $\mu$M A-SpA in *Mixture 1* in acetate buffer, was applied on each
218 slide. A reference was measured before applying the protein-containing droplet. After 30
219 minutes, the ASM was measured during the different washings steps.

220 2.7. CuAAC immobilization of A-MBP

The CuAAC coupling of 1 $\mu$M A-MBP was performed in *Mixture 1* in acetate buffer during 30 minutes after which the ASM of immobilized MBP was determined.

### 2.8. Physical adsorption and covalent EDC/NHS immobilization of SpA

For physical adsorption, PVC slides were put into a 1 $\mu$M SpA solution in Tris-NaCl buffer for 1.5 hours. For covalent surface coupling by EDC/NHS, carboxylated silicon slides were put into a solution of 0.2 M EDC and 0.071 M NHS in MES buffer for 1 h. Next, the slides were put into MES buffer containing 1 $\mu$M SpA for 1.5 h, followed by flushing with WB for several minutes and measuring the ASM in MES buffer. This procedure was performed in triplicates. After immobilization, the ASM on the slides was measured while flushing with Tris buffer. This procedure was again performed in triplicates.

### 2.9. Activity of immobilized SpA and MBP

It has been shown that adsorption can affect protein activity and due to random orientation of the molecules on the surface, binding sites may not be reachable [52-56]. Therefore, the effect of the immobilization methods on the activity, as measured by the interaction and binding to an antibody, was determined. The SpA covered slides, obtained *via* physical adsorption, EDC/NHS coupling or CuAAC chemistry were put into cuvettes containing PBS. For each slide a reference surface mass was recorded and human IgG (hIgG) was added to a final concentration of 0.33 $\mu$M. The interaction between the immobilized SpA and hIgG was monitored using real-time ellipsometry. Similarly, monoclonal anti-MBP (0.33 $\mu$M) was added to the cuvettes containing the MBP covered slides. The interaction between the antibody and immobilized MBP was monitored in real-time by ellipsometry.

## 3. Results and Discussion

### 3.1. Azidification and Alkynation

A covalent surface protein immobilization *via* CuAAC 'click' chemistry requires the introduction of two complementary functional groups, *i.e.* one on the silicon slide and the other in the protein. After the azidification of the carboxylated slides using EDC/NHS chemistry, the surface angle of water on the slides was measured. It was found that the contact angle changed from 0º (hydrophilic) to 32.4° (±2.9°) (more hydrophobic). This is in agreement with the expected modification of carboxylic acids to azides on the surface. It should be noted that at pH 4, parts of the remaining non-modified carboxylic groups will be negatively charged, resulting in an electrostatic attraction of the positively charged SpA (SpA: pI~5.4; theoretically calculated with Innovagen protein property calculator) and MBP (MBP: pI~5; idem) to the surface at which the 'click' reaction takes place [57,58].

In addition to the surface azidification, the proteins SpA and MBP were complementary functionalized with alkynes *via* the endogenous lysines. By alkynating the lysines, the pI of the global protein will decrease and this change can be visualized by native polyacrylamide gel electrophoresis (PAGE). Figure 2 illustrates the difference between wild-type SpA (left) and A-SpA (right) after performing native PAGE. At pH 8.8 the more negatively charged A-SpA migrates faster than SpA towards the positive pole, demonstrating a successful alkynation.

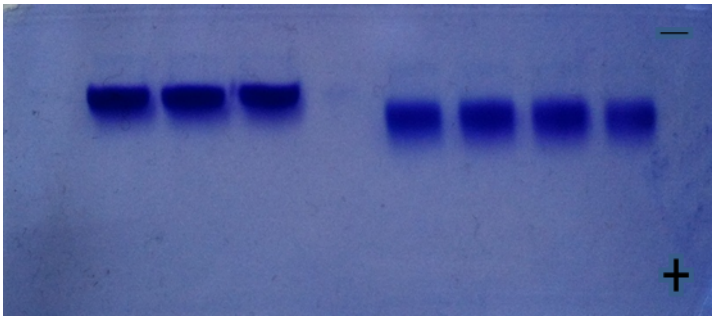


**Figure 2.** Native polyacrylamide gel electrophoresis of wild-type SpA (left, three replicate samples) and A-SpA (right, four replicate samples).

264 3.2. CuAAC Coupling with SpA

265 To find the optimal conditions for protein immobilization *via* CuAAC chemistry, SpA was
266 used as a model protein. The reaction conditions were tested using different (combinations of)
267 reducing agents (TCEP *versus* sodium L-ascorbate), ligands (water soluble THPTA *versus* the
268 apolar TBTA) and buffers (PBS pH 7.4 *versus* sodium acetate buffer pH 4). Figures 3 and 4
269 summarize the increase in surface mass as measured by ellipsometry for the different reaction
270 mixtures in PBS pH 7.4 and acetate buffer pH 4, respectively, after 18h. Each condition was
271 repeated on 8 replicate slides.

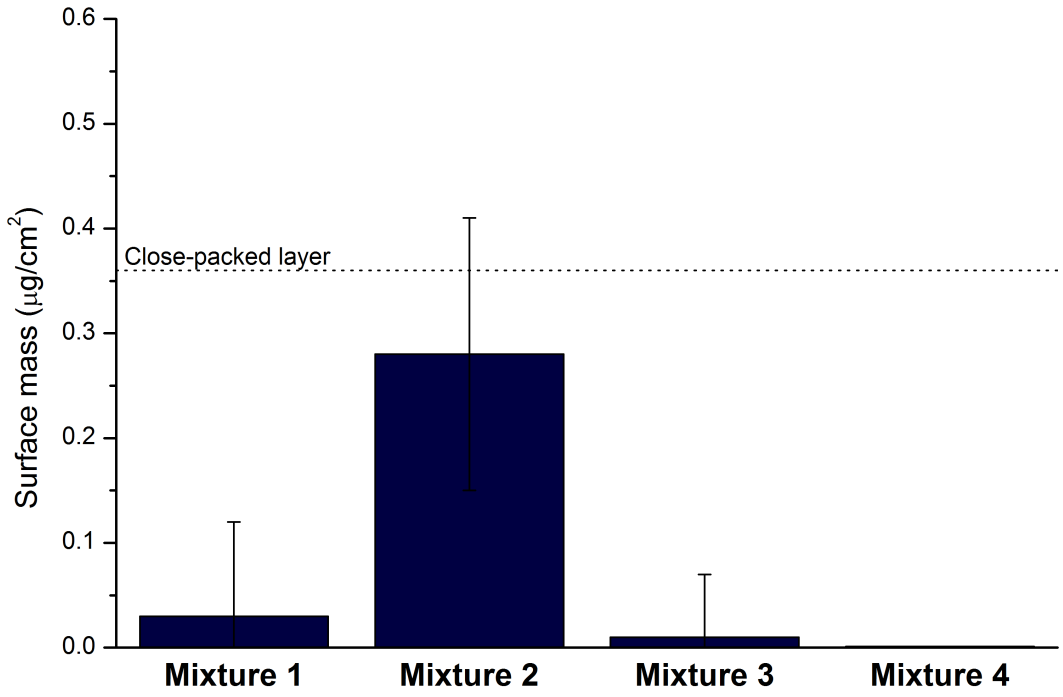


272

273 **Figure 3.** Surface mass of four different mixtures in PBS pH 7.4. The dashed
274 line marks the theoretical surface mass of a close-packed monolayer of SpA as
275 estimated by Lahiri et al [59].

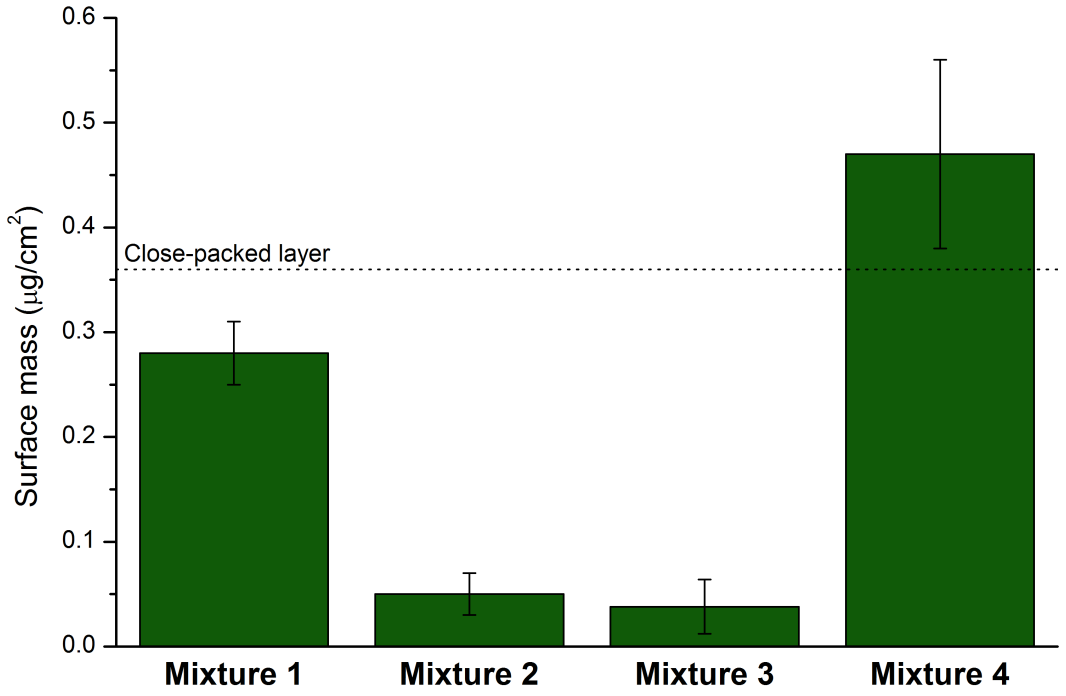


276

277 **Figure 4.** Surface mass of four different mixtures dissolved in sodium acetate
278 buffer pH 4. The dashed line marks the theoretical surface mass of a close-
279 packed monolayer of SpA as estimated by Lahiri et al [59].

280

281 When the CuAAC reaction was performed in PBS (pH 7.4) only reaction *Mixture 2* shows
282 a significant binding of 0.28 $\mu$g/cm$^2$. However, the reproducibility was rather poor with a
283 standard deviation of 46 %. For the sodium acetate buffer (pH 4) reactions in *Mixture 1* and
284 *Mixture 4* both yielded significant protein surface coverages of 0.28 $\mu$g/cm$^2$ and 0.47 $\mu$g/cm$^2$,
285 with standard deviations of 11 % and 19 %, respectively. The better reproducibility in
286 *Mixture 1* and *Mixture 4* at pH 4 can be explained by the attraction forces between the
287 positively charged proteins and the negative charges of the remaining carboxylate groups at
288 the substrate surface at this pH [56].

289 The maximum amount of protein that can be immobilized on a surface was estimated by a
290 theoretical model described by Lahiri et al [59]. This model estimates the theoretical maximal
291 number of protein molecules per $mm^2$ in a close-packed hexagonal monolayer arrangement.
292 With this model, the maximum surface coverage of SpA was estimated to be 0.36 $\mu g/cm^2$.

293 Although this is just a model estimate assuming the proteins are hard spheres of uniform
294 density, the three reaction conditions yielding the highest surface mass are close to this
295 theoretical value: *Mixture 2* in PBS and *Mixtures 1* and *Mixture 4* in acetate buffer. However,
296 *Mixture 2* in PBS and *Mixture 4* in acetate buffer both contain DMSO, an organic solvent
297 which might result in (partial) denaturation of proteins [60,61]. *Mixture 1* in acetate buffer is
298 the DMSO-free alternative of *Mixture 4* in the acetate buffer and is therefore chosen as the
299 optimal CuAAC reaction condition and is used for the subsequent reactions.

300 To test the stability of the CuAAC covalent coupling of A-SpA to the azidified surface in
301 *Mixture 1 in* acetate buffer, four experiments were simultaneously performed in which (non-)
302 alkynated SpA and/or non-azidified surfaces were used. Proteins were coupled to the surface
303 for 18 hours after which the surfaces were washed with different washing solutions. During
304 washing, the ASM was measured in real-time. Figure 5 shows that only A-SpA coupled to the
305 azidified silicon surface resisted the different washing steps. In the three control experiments
306 almost all protein is removed during washing. This suggests that the used CuAAC coupling
307 protocol of an alkynated protein to an azidified surface results in a stable and covalent bond.

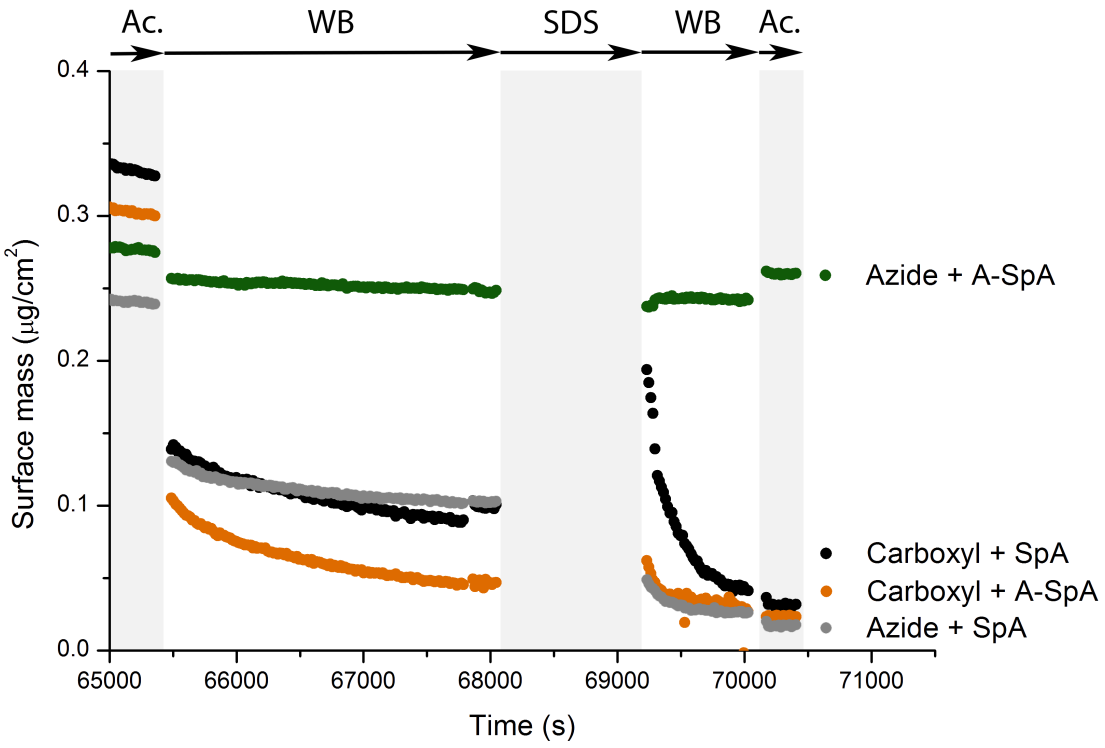


308

309 **Figure 5.** Surface mass evolution as measured by ellipsometry during
310 consecutive washing steps with acetate buffer (Ac.); washing buffer (WB);
311 sodium dodecyl sulfate solution (SDS); washing buffer and acetate buffer: for A-
312 SpA which is covalently coupled to azidified silicon slides by CuAAC with
313 *Mixture 1* in acetate buffer (green) and for control experiments accomplished
314 under identical conditions but with carboxylated plates and/or non-alkynated
315 SpA.

316

317 To test whether the immobilization reaction time could be shortened, surface mass
318 measurements were also performed at 1800 sec (30 minutes), since preliminary measurements
319 of the immobilization in acetate buffer showed a fast increase in surface mass during the first
320 30 minutes. Reaction times under 30 minutes are too short to get complete covalent coupling
321 and surface mass increase is mainly due to adsorption (data not shown). When using *Mixture*

*1* in acetate buffer, it was found that the formation of the A-SpA layer was already complete after 30 minutes, which is only 2.5% of the time that was presumed to be needed to obtain sufficient protein layers. On the other hand when using *Mixture 2* in PBS no signs of a biolayer in development could be observed after 30 minutes and a reaction time of 18 hours was needed to obtain a biolayer of comparable mass. In addition, *Mixture 2* in PBS leads to high standard deviations. This implies that *Mixture 1* in acetate buffer does not only enhances the rate of formation of the biofilm on the azide functionalized substrate but also leads to highly reproducible layers (table 2).

**Table 2.** Surface mass measurements and the corresponding standard deviations after 30 min and 18 h of CuAAC reaction. At 30 min, a 5 min wash step with WB was performed to see the difference in surface mass.

| **Time** | **Surface mass ($\mu$g/cm$^2$)** | | | |
|---|---|---|---|---|
| | **PBS** | **S.D.[1]** | **Acetate** | **S.D.[2]** |
| **0** | 0.00 | | 0.00 | |
| ↓ | ***CuAAC coupling reaction*** | | | |
| **30 min** | 0.00 | 0.01 | 0.35 | 0.02 |
| ↓ | ***Wash step with WB*** | | | |
| **35 min** | 0.00 | 0.01 | 0.33 | 0.01 |
| ↓ | ***CuAAC coupling reaction*** | | | |
| **18 h** | 0.38 | 0.18 | 0.37 | 0.03 |

[1]n=3, [2]n=4

The successful biofunctionalization of the silicon slide with proteins was supported by contact angle measurements. Whereas the azide functionalized slides exhibited an average water contact angle of 32.4° (±2.9°), this contact angle increased to 62.4° (±2.6°) after treatment with A-SpA using *Mixture 1* in acetate buffer. This is an indication of the chemical change caused by the formation of the A-SpA layer. Based on these experiments it can be

concluded that *Mixture 1* in acetate buffer results in an optimal and reproducible coupling of A-SpA to the azidified substrate in a short reaction time of 30 minutes.

### 3.3. Concentration Dependency of the CuAAC Coupling

Considering the future development of biofunctionalized surfaces based on antibodies, reducing the amount of protein/antibody per sample is highly recommended. Therefore, five additional protein concentrations (0.034, 0.068, 0.102, 0.136 and 0.500 $\mu$M) were tested for immobilization. After 30 minutes of immobilization in *Mixture 1* in acetate buffer, a surface mass of 0.08 $\mu$g/cm$^2$ was achieved for the 0.034 $\mu$M solution. In case of the 0.068 $\mu$M A-SpA 0.15$\mu$g/cm$^2$ was achieved and 0.17 $\mu$g/cm$^2$ for the 0.102 $\mu$M A-SpA. The 0.136 $\mu$M A-SpA solution reached a maximum of 0.20 $\mu$g/cm$^2$ and 0.25 $\mu$g/cm$^2$ was obtained by using a 0.5 $\mu$M A-SpA solution (Figure 6, top right).

The measurements confirm the effect of the protein concentration on the final protein mass of the biolayers (Figure 6). Varying the protein concentrations from 0 to 0.102 $\mu$M results in a very steep increase in A-SpA surface mass. Further raising the A-SpA concentration results in a gradual increase in surface mass and apparent saturation around 0.30 $\mu$g/cm$^2$. This amount is in agreement with the theoretical maximum amount of SpA that can be immobilized on a surface, i.e. 0.36 $\mu$g/cm$^2$ as estimated by a theoretical model described by Lahiri et al. [59].

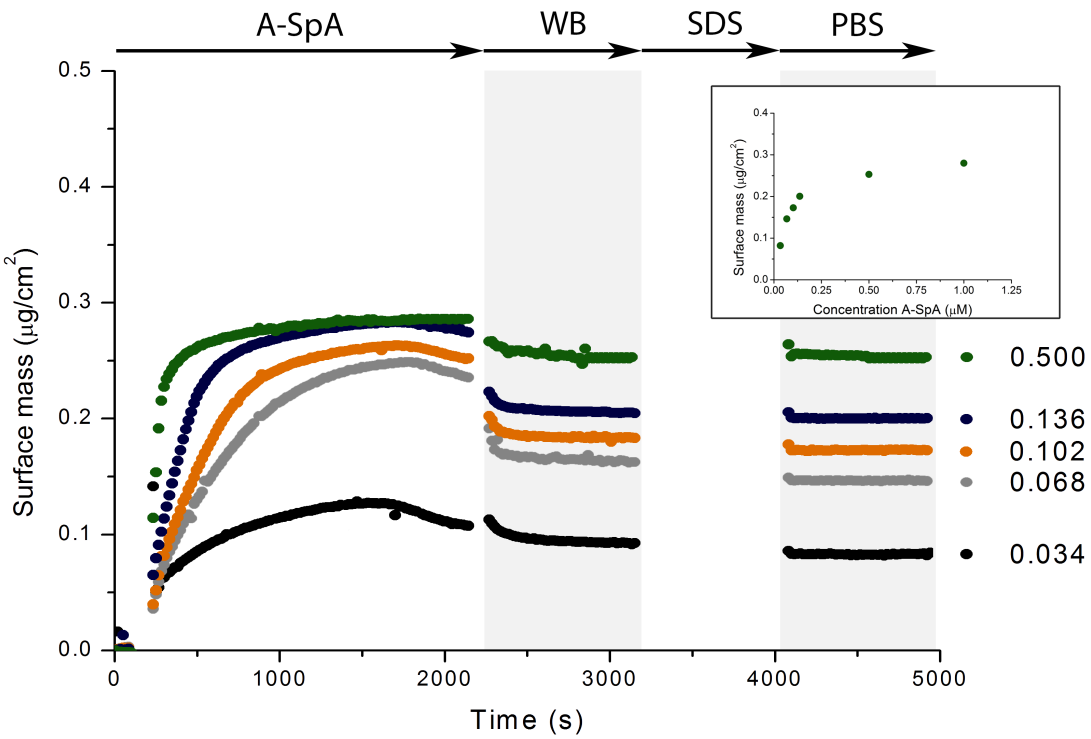


356

357 **Figure 6.** A-SpA Surface Mass evolution of CuAAC coupling using different
358 protein concentrations, followed by subsequent washing steps with WB, SDS and
359 PBS. The insert shows the concentration dependency of the final A-SpA surface
360 mass.

361

362 Lowering the concentration of the reaction mixture therefore results in a lower amount of
363 protein on the substrate. Higher protein concentrations are therefore preferred to create
364 maximally covered surfaces.

365 Another option to reduce protein consumption would be reducing the immobilization
366 reaction volume. By using the drop method, a 1 $\mu$M A-SpA solution in Mixture 1 in acetate
367 buffer was used, but the reaction volume was reduced from 400 $\mu$l (maximum volume
368 cuvettes) to 30 $\mu$l, the minimal volume to fully cover the same area of the azide-
369 functionalized silicon slides. Interestingly, this 13 times reduction in reaction volume still

results in protein layers of 0.29 ± 0.03 $\mu$g/cm$^2$ A-SpA. This means a considerable reduction in protein usage to obtain dense A-SpA layers which gives the opportunity to efficiently use higher protein concentrations to get optimal surface coverage.

### 3.4. Comparison with other immobilizing methods

The optimized surface CuAAC coupling of A-SpA was compared to other commonly used coupling procedures as shown in Figure 7. The ASM of 0.28 $\mu$g/cm$^2$ resulting from the CuAAC reaction matches a surface coverage of 78% of a close packed monolayer of 0.36 $\mu$g/cm$^2$ (Lahiri et al. [59]). For EDC/NHS coupling and physical adsorption, this is only 61% and 53%, respectively. Comparing the results of the EDC/NHS coupling of 1 $\mu$M SpA (0.22 +/- 0.02 $\mu$g/cm$^2$) with the results from Figure 6, it is remarkable that a 0.136 $\mu$M solution used in combination with the CuAAC coupling yields comparable surface mass (0.20 $\mu$g/cm$^2$), even though the reaction time is 5 times less and the protein concentration is 7 times less. One explanation for this immobilization efficiency and higher surface mass after click reaction compared to EDC/NHS might be that when SpA is modified with an alkyne, a spacer was also introduced (Figure 1). This linker creates a suitable separation between the surface and the protein. This might reduce steric hindrance, leading to increased immobilization mass. Hence, this indicates that CuAAC based immobilization leads to a considerable improvement in reproducibility and surface mass.

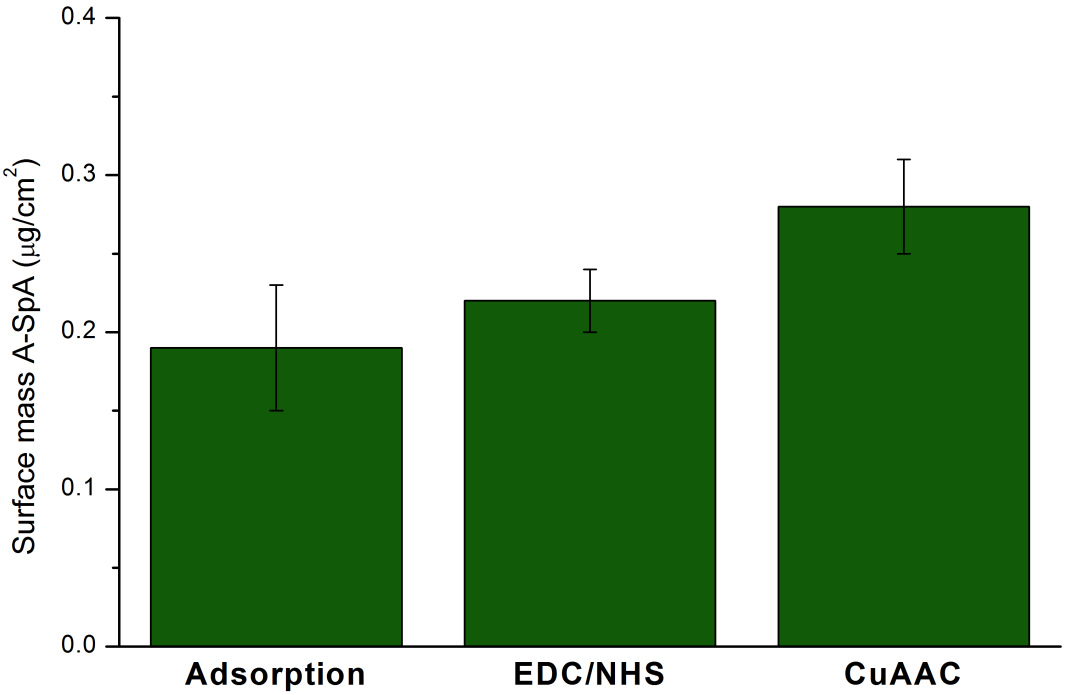


388

389 **Figure 7.** Average Surface Mass (ASM) and standard deviation obtained from
390 immobilizations of SpA on carboxylated silicon slides by physical adsorption and
391 EDC/NHS coupling and of A-SpA on azidified slides with CuAAC.

392

393 3.5. Activity measurements of immobilized SpA

394 By measuring the binding of human IgG to the immobilized SpA, the activity of the
395 proteins after surface coupling *via* CuAAC, EDC/NHS or physical adsorption has been
396 evaluated (Figure 8).

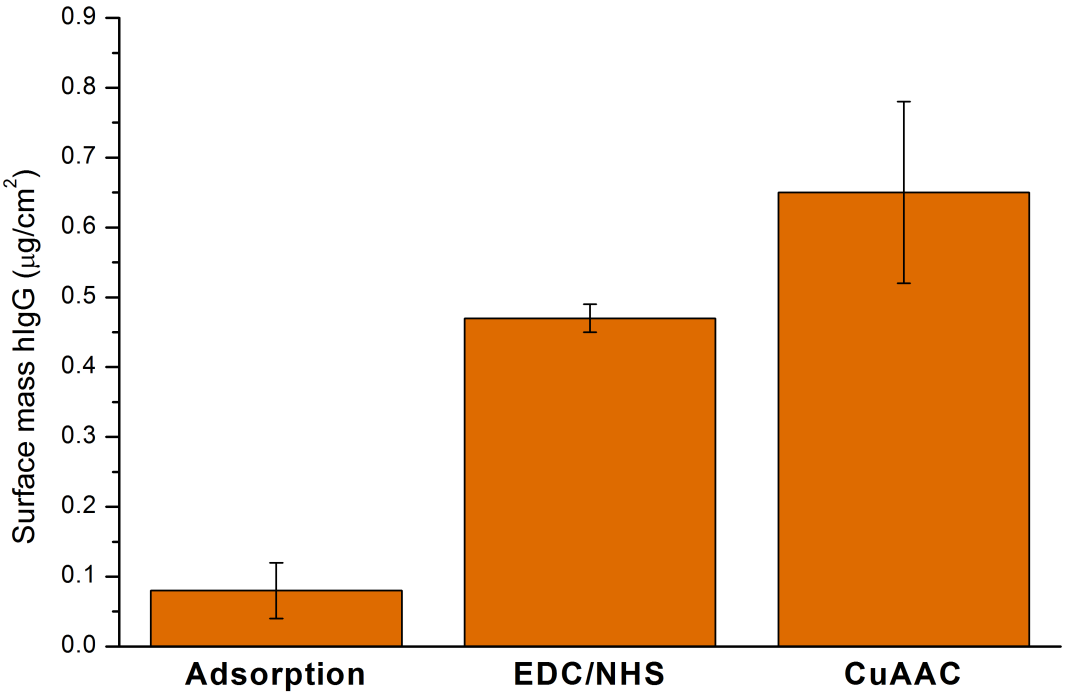


397

398 **Figure 8.** Average Surface Mass (ASM) of antibody and corresponding
399 standard deviations obtained after binding of human IgG to different SpA
400 functionalized slides.

401

402 The physically adsorbed SpA is able to bind only minute amounts of hIgG, *i.e.* 0.08
403 $\mu$g/cm$^2$. The hIgG density of EDC/NHS coupled SpA is 0.47 $\mu$g/cm$^2$. The highest amount of
404 hIgG binding, *i.e.* 0.65 $\mu$g/cm$^2$, can be observed for A-SpA layers immobilized by CuAAC.
405 This mass increase of hIgG is two times higher than a side-on close packed hIgG monolayer,
406 *i.e.* 0.3 $\mu$g/cm$^2$, and is more than 40% of fully end-on covered hIgG monolayer, *i.e.* 1.5
407 $\mu$g/cm$^2$ [62]. This indicates that the surface consists of a mixture of sideway oriented and end-
408 on oriented hIgG molecules. After hIgG binding, the slides were flushed with an acidic
409 glycine solution, a procedure often used to only break the specific antibody-antigen
410 interactions in antibody purification columns [63]. After washing, the original layers of 0.28

411 $\mu$g/cm$^2$ were restored demonstrating the very specific binding between A-SpA and hIgG. The
412 possibility of aspecific binding is reduced due to the obtained dense A-SpA layer (78% of
413 close-packed), which does not allow for much 'protein-free' spaces in the biofilm. These gaps
414 could be a possible cause for increased aspecific binding of the antibody.

415 To further study the impact of surface coverage on the hIgG binding capacity of the A-
416 SpA, different slides with increasing A-SpA surface mass was tested. The slides incubated
417 with different A-SpA concentrations (figure 6) were incubated with hIgG and the antibody
418 binding was followed (figure 9).

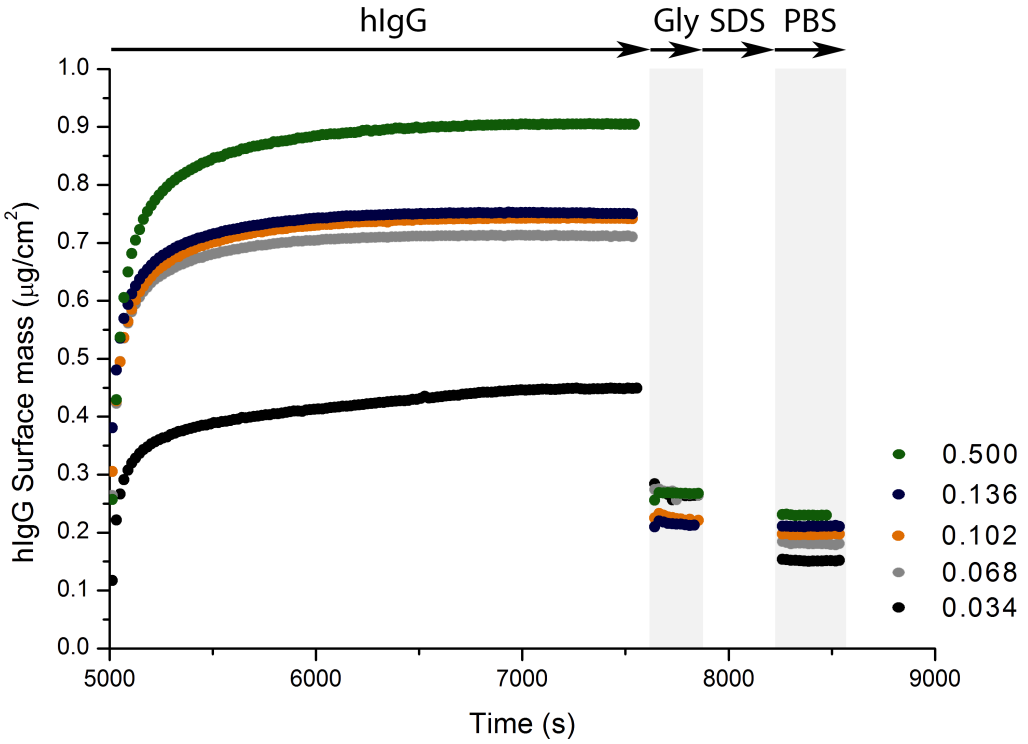


419

420 **Figure 9.** hIgG Surface Mass evolution after binding to surfaces with different
421 amounts of A-SpA. The binding of hIgG is followed by washing with glycine,
422 SDS and PBS.

423

The binding capacity towards hIgG increases with the increasing A-SpA surface mass, indicating that the improved coverage with A-SpA has a direct positive impact on the binding capacity of hIgG. Further it can be seen that the higher the initial amount of immobilized A-SpA on the azide surface is (before adding IgG), the less aspecific adsorbed IgG needs to be removed by SDS after completion of the glycine washing step. This probably originates from the fact that a lower density of the initial A-SpA layers can offer the opportunity for aspecific adsorption of IgG molecules to the 'protein-free' substrate (*vide supra*). As a result, it can be concluded that the increased SpA surface mass (0.28 $\mu$g/cm$^2$) obtained *via* CuAAC, not only leads to an increased presence of receptor (SpA) molecules on the surface (see figure 6), but also has the advantage of reducing aspecific binding of target molecules, in this case hIgG, to the underlying substrate. This will have a positive impact on the signal-to-noise ratio when applying this CuAAC coupling technique in sensing devices, thus improving their sensitivity and decreasing the chance of possible errors.

### 3.6. Covalent coupling of MBP

To confirm that the results obtained for SpA are representative for and applicable to other protein systems, experiments were repeated with MBP. The use of CuAAC with *Mixture 1* in acetate buffer for 30 minutes resulted in the following covalently coupled biolayers (Figure 10). For A-MBP, an average surface mass of 0.21 $\mu$g/cm$^2$ ± 0.033 $\mu$g/cm$^2$ was obtained (n=3). Upon coupling fully alkynated MBP, an average surface mass of 0.25 $\mu$g/cm$^2$ ± 0.07 $\mu$g/cm$^2$ was obtained (n=3). These results clearly demonstrate the covalent attachment of MBP. Although higher surface mass was obtained for the fully alkynated MBP, this full alkynation affects the antibody binding (*vide infra*).

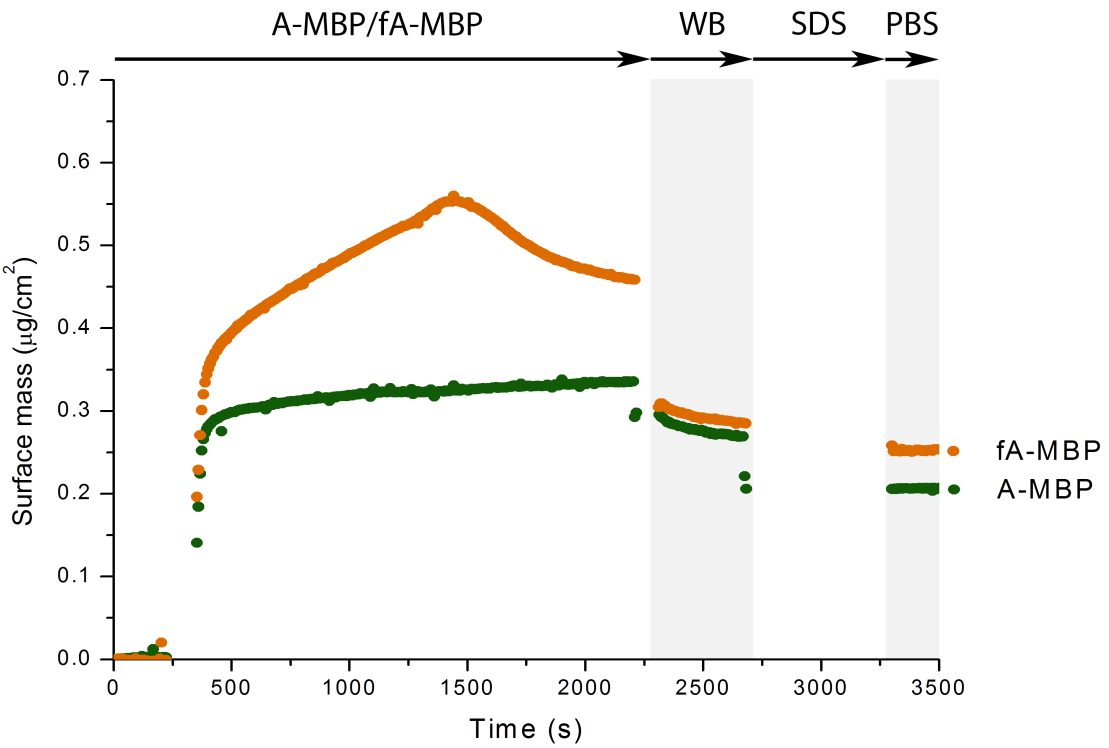


446

447 **Figure 10.** Surface mass evolution for the coupling of standard alkynated MBP (green)
448 and fully alkynated MBP (orange) to azidified silicon slides by CuAAC with *Mixture 1* and
449 for consecutive washing steps with washing buffer (WB), sodium dodecyl sulfate solution
450 (SDS) and PBS.

451 3.7. Activity measurements of MBP

452 The MBP covered slides were incubated with anti-MBP. Figure 11 shows a remarkable
453 difference between both immobilization types in terms of activity. Despite the fact that the
454 surface coverage of fA-MBP is almost 25% higher than that of A-MBP (Figure 10), the A-
455 MBP coated slides bind significant higher amounts of anti-MBP antibody i.e. 0.13 $\mu$g/cm$^2$
456 compared to only 0.05 $\mu$g/cm$^2$ for fA-MBP. This might indicate that the high number of
457 modifications causes conformational changes in the protein. This will lead to reduced
458 accessibility by anti-MBP antibodies and therefore less binding. Obviously, it is important to
459 minimize the number of modifications in order to prevent (conformational) changes that can

lead to reduced protein activity. Moving towards partial or even single and eventually to a site-specific functionalization of the protein of interest can offer the possibility to modify and immobilize the protein in a controllable way without interfering with its functioning. This way, biomaterial with optimal biological activity can be created.

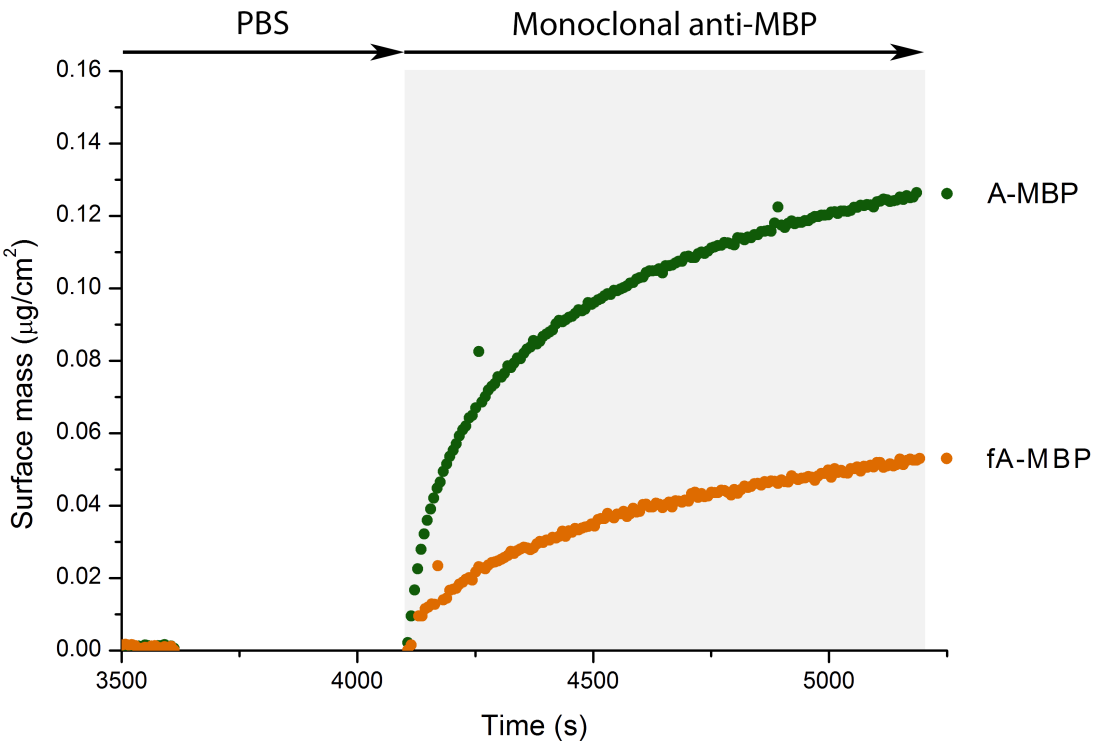


**Figure 11.** Surface mass evolution of the MBP-coupled slides during the binding of monoclonal anti-MBP: standard alkynated A-MBP (green; average increase: 0.13 $\mu$g/cm²) and fully alkynated fA-MBP (orange; average increase: 0.05 $\mu$g/cm²).

## 4. Conclusions

The covalent coupling of SpA and MBP on azide functionalized silicon slides has been achieved *via* an optimized copper catalyzed azide-alkyne cycloaddition. For this optimization,

the immobilization of the proteins was followed in real-time with *in situ* ellipsometry. This allowed us to study the click reaction in a time-dependent manner and to find the optimal reaction time and conditions to create covalently coupled protein surfaces with an optimal protein coverage and subsequent activity. An effective, reproducible and rapid method has been developed by combining copper sulfate, sodium ascorbate and THPTA in 0.01 M sodium acetate buffer at pH 4 in 30 minutes. Furthermore, a considerably improved surface mass was obtained as compared to other commonly used coupling techniques demonstrating its innovative potential for future biofunctionalization of surfaces. After coupling, the biolayers kept their characteristics, *i.e.* the bound SpA was still able to interact with human IgG and the bound MBP with MBP antibody. These results confirm that this covalent coupling method can be used for different proteins without inhibiting their corresponding activity. At the same time the increased surface mass resulted in a reduction in aspecific binding of target molecules. This rapid and covalent coupling strategy to a solid carrier offers promising prospects for a wide range of applications based on biofunctionalized surfaces, *i.e.* biofunctionalized microarrays and biosensing devices.

**Acknowledgements**

The authors acknowledge financial support from the special research fund (BOF). This study was a part of the Interreg IV-A project "BioMiMedics" (www.biomimedics.org). In the framework of Interreg IV-A, the financial contribution from the EU and the province Limburg (Belgium) is kindly acknowledged. We further acknowledge the financial support from the Interuniversity Attraction Poles Programme (P7/05) initiated by the Belgian Science Policy Office (BELSPO).

**Biographies**

**Tom Vranken** received his Master degree in Biomedical Sciences (Bioelectronics and Nanotechnology) at University of Hasselt, Belgium, in 2010. He did his Ph.D. thesis under supervision of Prof. Dr. Thomas Cleij where he performed research in order to develop a reliable and reproducible protein immobilization method towards the development of biofunctionalized surfaces for divers purposes.

**Erik Steen Redeker** obtained his Master's degree in chemistry, with a specialism in biochemistry, at the Utrecht University and his Ph.D. in Sciences at the Antwerp University. In 2008 he was appointed as a postdoctoral fellow at the Hasselt University where he co-founded the Biomolecule Design Group. He is currently appointed at the Maastricht University as a lecturer and member of the research group in Nano(Bio)Technology and Bio-Electronics. His research is focused on the rational (re)design, development and (bio)synthesis of biopolymers. He uses synthetic biology approaches and other techniques inspired by and derived from strategies found in nature.

**Adam Miszta** Since 2012 Dr Miszta has been working in the field of thrombosis and haemostasis with the Von Willeband Factor, thrombin generation and fibrinolysis as special

512 interest. Previously he worked in the field of Protein-membrane interactions at the J.
513 Heyrovsky Institute of Physical Chemistry of Czech Academy of Sciences in Prague. After
514 moving to Maastricht he worked as a Senior Scientist at the Maastricht University and at
515 Delbia bv. Currently he works as a scientist at the University of Maastricht and at Synapse
516 Research Institute. He published several papers in the field of protein-membrane interactions
517 measured with ellipsometry.

518 **Brecht Billen** received his Master Degree in Bioelectronics and Nanotechnology at Hasselt
519 University in 2012. Currently, he is a PhD-student at the Institute for Materials Research
520 (IMO) of Hasselt University. He is part of the Biomolecule Design Group and his current
521 research is focused on the site-specific functionalization of proteins.

522 **Wim Hermens** studied theoretical physics at the University of Amsterdam, where he
523 graduated in 1968. In 1971 he obtained his PhD degree at the same university for a thesis on
524 chemical reactions in neutron stars. In the meantime he worked at Leiden University on
525 ellipsometry, an optical technique for measurement of physico-chemical processes at
526 interfaces. In 1974 he moved to the medical faculty of the new Maastricht University, where
527 he worked on membrane-protein interactions in blood coagulation. In 1996 he became
528 professor of molecular physics at Maastricht University and he retired from active research in
529 2013.

530 **Bas de Laat** Since 2001 Dr. de Laat has been working in the field of thrombosis and
531 haemostasis with the antiphospholipid syndrome, Von Willeband Factor and thrombin
532 generation as special interest. After working at the University Medical Center Utrecht and
533 Sanquin Blood Supply Amsterdam Dr. de Laat is currently associate professor at the
534 University of Maastricht and general director of Synapse Research Institute. Dr. de Laat has
535 received several grants in his career and his work is acknowledged by the Dutch Heart

536 foundation as he received 2 consecutive fellowships. Dr. de Laat serves as reviewer for
537 several journals including Blood, Lancet and New England Journal of Medicine.

538 **Peter Adriaensens** Peter Adriaensens graduated in 1990 from UHasselt University, Belgium
539 with a PhD on biopolymer NMR research. Subsequently, he was appointed as permanent
540 researcher/lecturer. In 2007 he was appointed Professor at Hasselt University, where he joins
541 the departments of Organic and (Bio)Polymer Chemistry and Applied and Analytical
542 Chemistry. Generally, his research focuses on the site-specific “click” functionalization of
543 nanobody proteins towards a covalent and oriented coupling to diverse surfaces for
544 applications in the field of biohybrid particles and materials.

545 **Wanda Guedens** received her PhD degree in chemistry in 1999 from Hasselt University,
546 Belgium where she was appointed as assistant professor in 2004 at the Chemistry
547 Department. From 2015 she is a professor of (bio)chemistry. Currently, she is heading the
548 multidisciplinary research in biochemical and biomedical nanotechnology in the Biomolecule
549 Design Group at the Institute of Materials Research at Hasselt University. Her research
550 concentrates on the controlled biofunctionalization of surfaces for innovative biomaterials.
551 More specifically, the site-specific nanobody modification towards an oriented and covalent
552 coupling to functionalized substrates such as conjugated polymers, (nano) diamond, graphene
553 and nanoparticles using 'click' chemistry.

554 **Thomas J. Cleij** obtained his PhD in chemistry at Utrecht University. Subsequently he was
555 appointed as assistant professor at Louisiana State University and associate and full professor
556 at Hasselt University. Since 2012, he has been appointed at Maastricht University as a Full
557 Professor of chemistry. Since 2015 he is also Dean Sciences at this university. The expertise
558 of his research group in Nano(Bio)Technology and Bio-Electronics focuses on the
559 combination and interplay of novel functional polymeric materials and advanced applications

in the life sciences, such as biosensors. He has published about 100 papers on polymeric materials science and engineering.

## References


[1] C.A.K. Borrebaeck, C. Wingren, Design of high-density antibody microarrays for disease proteomics: key technological issues, J Proteomics. 72 (2009) 928–935. doi:10.1016/j.jprot.2009.01.027.

[2] T.R.J. Holford, F. Davis, S.P.J. Higson, Recent trends in antibody based sensors, Biosens. Bioelectron. 34 (2012) 12–24. doi:10.1016/j.bios.2011.10.023.

[3] F. Li, W. Chen, S. Zhang, Development of DNA electrochemical biosensor based on covalent immobilization of probe DNA by direct coupling of sol-gel and self-assembly technologies, Biosens. Bioelectron. 24 (2008) 787–792. doi:10.1016/j.bios.2008.06.052.

[4] Z.-H. Wang, G. Jin, Covalent immobilization of proteins for the biosensor based on imaging ellipsometry, J Immunol Methods. 285 (2004) 237–243. doi:10.1016/j.jim.2003.12.002.

[5] D. Van der Voort, C.A. McNeil, R. Renneberg, J. Korf, W.T. Hermens, J.F.C. Glatz, Biosensors: basic features and application for fatty acid-binding protein, an early plasma marker of myocardial injury, Sensor Actuat B-Chem. 105 (2004) 50–59. doi:10.1016/j.snb.2004.02.035.

[6] P.D. Skottrup, M. Nicolaisen, A.F. Justesen, Towards on-site pathogen detection using antibody-based sensors, Biosensors and Bioelectronic. 24 (2007) 339–348. doi:10.1016/j.bios.2008.06.045.

[7] D. Chen, M. Davis, Molecular and functional analysis using live cell microarrays, Curr. Opin. Chem. Biol. 10 (2006) 28–34. doi:10.1016/j.cbpa.2006.01.001.

[8] M.P. Byfield, R.A. Abuknesha, Biochemical aspects of biosensors, Biosensors and Bioelectronic. 9 (1994) 373–400. doi:10.1016/0956-5663(94)80038-3.

[9] B.M. Paddle, Biosensors for chemical and biological agents of defence interest, Biosensors and Bioelectronic. 11 (1996) 1079–1113. doi:10.1016/0956-5663(96)82333-5.

[10] Y. Lei, W. Chen, A. Mulchandani, Microbial biosensors, Anal. Chim. Acta. 568 (2005) 200–210. doi:10.1016/j.aca.2005.11.065.

[11] S. Mun, S.-J. Choi, Optimization of the hybrid bilayer membrane method for immobilization of avidin on quartz crystal microbalance, Biosens. Bioelectron. 24 (2009) 2522–2527. doi:10.1016/j.bios.2009.01.006.

[12] M.A. Skidmore, S.J. Patey, N.T.K. Thanh, D.G. Fernig, J.E. Turnbull, E.A. Yates, Attachment of glycosaminoglycan oligosaccharides to thiol-derivatised gold surfaces, Chem Commun (Camb). (2004) 2700–2701. doi:10.1039/b411726c.

[13] F. Horemans, A. Weustenraed, D. Spivak, T.J. Cleij, Towards water compatible MIPs for sensing in aqueous media, J. Mol. Recognit. 25 (2012) 344–351. doi:10.1002/jmr.2191.

[14] F. Horemans, H. Diliën, P. Wagner, T.J. Cleij, MIP-based Sensor Platforms for Detection of Analytes in Nano- and Micromolar Range, in: S. Li, Y. Ge, S.A. Piletsky (Eds.), Molecularly Imprinted Sensors, Elsevier B.V, 2012: pp. 91–124. doi:10.1016/B978-0-444-56331-6.00005-0.

[15] D. Jiang, J. Tang, B. Liu, P. Yang, X. Shen, J. Kong, Covalently coupling the antibody on an amine-self-assembled gold surface to probe hyaluronan-binding protein with capacitance measurement, Biosensors and Bioelectronic. 18 (2003) 1183–1191. doi:10.1016/S0956-5663(02)00253-1.
[16] S. Susmel, R. Toniolo, A. Pizzariello, N. Dossi, G. Bontempelli, A piezoelectric immunosensor based on antibody entrapment within a non-totally rigid polymeric film, Sensor Actuat B-Chem. 111 (2004) 331–338. doi:10.1016/j.snb.2004.11.052.
[17] M. Köhn, Immobilization strategies for small molecule, peptide and protein microarrays, J. Peptide Sci. 15 (2009) 393–397. doi:10.1002/psc.1130.
[18] J.E. Gautrot, W.T.S. Huck, M. Welch, M. Ramstedt, Protein-resistant NTA-functionalized polymer brushes for selective and stable immobilization of histidine-tagged proteins, ACS Appl. Mater. Interfaces. 2 (2010) 193–202. doi:10.1021/am9006484.
[19] E. Briand, M. Salmain, C. Compère, C.-M. Pradier, Immobilization of Protein A on SAMs for the elaboration of immunosensors, Colloids and Surfaces B: Biointerfaces. 53 (2006) 215–224. doi:10.1016/j.colsurfb.2006.09.010.
[20] Y. Gao, I. Kyratzis, Covalent immobilization of proteins on carbon nanotubes using the cross-linker 1-ethyl-3-(3-dimethylaminopropyl)carbodiimide--a critical assessment, Bioconjugate Chem. 19 (2008) 1945–1950. doi:10.1021/bc800051c.
[21] E. Steen Redeker, D.T. Ta, D. Cortens, B. Billen, W. Guedens, Peter Adriaensens, Protein engineering for directed immobilization, Bioconjugate Chem. 24 (2013) 1761–1777. doi:10.1021/bc4002823.
[22] L.S. Wong, F. Khan, J. Micklefield, Selective covalent protein immobilization: strategies and applications, Chem. Rev. 109 (2009) 4025–4053. doi:10.1021/cr8004668.
[23] L.S. Wong, J. Thirlway, J. Micklefield, Direct site-selective covalent protein immobilization catalyzed by a phosphopantetheinyl transferase, J. Am. Chem. Soc. 130 (2008) 12456–12464. doi:10.1021/ja8030278.
[24] S.H. North, E.H. Lock, C.J. Cooper, J.B. Franek, C.R. Taitt, S.G. Walton, Plasma-based surface modification of polystyrene microtiter plates for covalent immobilization of biomolecules, ACS Appl. Mater. Interfaces. 2 (2010) 2884–2891. doi:10.1021/am100566e.
[25] J.E. Butler, L. Ni, R. Nessler, K.S. Joshi, M. Suter, B. Rosenberg, et al., The physical and functional behavior of capture antibodies adsorbed on polystyrene, J Immunol Methods. 150 (1992) 77–90.
[26] R.K. Iha, K.L. Wooley, A.M. Nyström, D.J. Burke, M.J. Kade, C.J. Hawker, Applications of orthogonal "click" chemistries in the synthesis of functional soft materials, Chem. Rev. 109 (2009) 5620–5686. doi:10.1021/cr900138t.
[27] J.A. Prescher, C.R. Bertozzi, Chemistry in living systems, Nat. Chem. Biol. 1 (2005) 13–21. doi:10.1038/nchembioo605-13.
[28] L. Nebhani, C. Barner-Kowollik, Orthogonal Transformations on Solid Substrates: Efficient Avenues to Surface Modification, Adv. Mater. 21 (2009) 3442–3468. doi:10.1002/adma.200900238.
[29] L. Liang, D. Astruc, The copper(I)-catalyzed alkyne-azide cycloaddition (CuAAC) "click" reaction and its applications. An overview, Coordination Chemistry Reviews. 255 (2010) 2933–2945. doi:10.1016/j.ccr.2011.06.028.
[30] A.C. Gouget-Laemmel, J. Yang, M.A. Lodhi, Functionalization of azide-terminated silicon surfaces with glycans using click chemistry: XPS and FTIR study, J. Phys. Chem. C. 117 (2013) 368–375. doi:10.1021/jp309866d.
[31] B. Malvi, B.R. Sarkar, D. Pati, R. Mathew, "Clickable" SBA-15 mesoporous

materials: synthesis, characterization and their reaction with alkynes, J. Mater. Chem. 19 (2009) 140–14169. doi:10.1016/S1077-9108(08)79172-2.
[32] P.K.B. Palomaki, P.H. Dinolfo, Structural analysis of porphyrin multilayer films on ITO assembled using copper(I)-catalyzed azide-alkyne cycloaddition by ATR IR, ACS Appl. Mater. Interfaces. 3 (2011) 4703–4713. doi:10.1021/am201125p.
[33] J.-S. Seo, S. Lee, C.D. Poulter, Regioselective covalent immobilization of recombinant antibody-binding proteins a, g, and L for construction of antibody arrays, J. Am. Chem. Soc. 135 (2013) 8973–8980. doi:10.1021/ja402447g.
[34] F. Bally, K. Cheng, H. Nandivada, X. Deng, A.M. Ross, A. Panades, et al., Co-immobilization of biomolecules on ultrathin reactive chemical vapor deposition coatings using multiple click chemistry strategies, ACS Appl. Mater. Interfaces. 5 (2013) 9262–9268. doi:10.1021/am401875x.
[35] C. Uttamapinant, A. Tangpeerachaikul, S. Grecian, S. Clarke, U. Singh, P. Slade, et al., Fast, cell-compatible click chemistry with copper-chelating azides for biomolecular labeling, Angew. Chem., Int. Ed. 51 (2012) 5852–5856. doi:10.1002/anie.201108181.
[36] J.E. Moses, A. Moorhouse, The growing applications of click chemistry, Chem Soc Rev. 36 (2007) 1249–1262.
[37] M. King, A. Wagner, Developments in the field of bioorthogonal bond forming reactions-past and present trends, Bioconjugate Chem. 25 (2014) 825–839. doi:10.1021/bc500028d.
[38] V.P. Hong, N.F. Steinmetz, M. Manchester, M.G. Finn, Labeling live cells by copper-catalyzed alkyne--azide click chemistry, Bioconjugate Chem. 21 (2010) 1912–1916. doi:10.1021/bc100272z.
[39] N.J. Agard, J.A. Prescher, C.R. Bertozzi, A strain-promoted [3 + 2] azide-alkyne cycloaddition for covalent modification of biomolecules in living systems, J. Am. Chem. Soc. 126 (2004) 15046–15047. doi:10.1021/ja044996f.
[40] C.S. McKay, M.G. Finn, Click chemistry in complex mixtures: bioorthogonal bioconjugation, Chem. Biol. 21 (2014) 1075–1101. doi:10.1016/j.chembiol.2014.09.002.
[41] T.R. Chan, R. Hilgraf, K.B. Sharpless, V.V. Fokin, Polytriazoles as copper(I)-stabilizing ligands in catalysis, Org Lett. 6 (2004) 2853–2855. doi:10.1021/ol0493094.
[42] V.P. Hong, S.I. Presolski, C. Ma, M.G. Finn, Analysis and optimization of copper-catalyzed azide-alkyne cycloaddition for bioconjugation, Angew. Chem., Int. Ed. 48 (2009) 9879–9883. doi:10.1002/anie.200905087.
[43] C.P. Ramil, Q. Lin, Bioorthogonal chemistry: strategies and recent developments, Chem. Commun. 49 (2013) 11007–11022. doi:10.1039/c3cc44272a.
[44] M.I. Austermuhle, J.A. Hall, C.S. Klug, A.L. Davidson, Maltose-binding protein is open in the catalytic transition state for ATP hydrolysis during maltose transport, J Biol Chem. 279 (2004) 28243–28250. doi:10.1074/jbc.M403508200.
[45] E. Steen Redeker, D.T. Ta, D. Cortens, B. Billen, W. Guedens, Peter Adriaensens, Protein Engineering For Directed Immobilization, Bioconjugate Chem. 24 (2013) 1761–1777. doi:10.1021/bc4002823.
[46] C.W.N. Damen, H. Speijer, W.T. Hermens, J.H.M. Schellens, H. Rosing, J.H. Beijnen, The bioanalysis of trastuzumab in human serum using precipitate-enhanced ellipsometry, Anal. Biochem. 393 (2009) 73–79. doi:10.1016/j.ab.2009.06.006.
[47] N.S. Hatzakis, H. Engelkamp, K. Velonia, J. Hofkens, P.C.M. Christianen, A. Svendsen, et al., Synthesis and single enzyme activity of a clicked lipase-BSA hetero-dimer, Chem Commun (Camb). 19 (2006) 2012–2014. doi:10.1039/b516551b.

[48] B. Jagadish, R. Sankaranarayanan, L. Xu, R. Richards, J. Vagner, V.J. Hruby, et al., Squalene-derived flexible linkers for bioactive peptides, Bioorg. Med. Chem. Lett. 17 (2007) 3310–3313. doi:10.1016/j.bmcl.2007.04.001.
[49] S. Kalkhof, A. Sinz, Chances and pitfalls of chemical cross-linking with amine-reactive N-hydroxysuccinimide esters, Anal. Bioanal. Chem. 392 (2008) 305–312.
[50] E. Basle, N. Joubert, M. Pucheault, Protein Chemical Modification on Endogenous Amino Acids, Chem. Biol. 17 (2010) 213–227. doi:10.1016/j.chembiol.2010.02.008.
[51] P. Duplay, H. Bedouelle, A. Fowler, I. Zabin, W. Saurin, M. Hofnung, Sequences of the malE gene and of its product, the maltose-binding protein of Escherichia coli K12, J Biol Chem. 259 (1984) 10606–10613.
[52] M. Aizawa, K. Yun, T. Haruyama, Y. Yanagida, Protein engineering for self-assembling antibody molecules in an oriented manner, Supramolecular Science. 5 (1998) 761–764.
[53] I.-H. Cho, E.-H. Paek, H. Lee, J.Y. Kang, T.S. Kim, S.-H. Paek, Site-directed biotinylation of antibodies for controlled immobilization on solid surfaces, Anal. Biochem. 365 (2007) 14–23. doi:10.1016/j.ab.2007.02.028.
[54] R. Iwata, R. Satoh, Y. Iwasaki, K. Akiyoshi, Covalent immobilization of antibody fragments on well-defined polymer brushes via site-directed method, Colloids and Surfaces B: Biointerfaces. 62 (2008) 288–298. doi:10.1016/j.colsurfb.2007.10.018.
[55] S.R. Ahmed, A.T. Lutes, T.A. Barbari, Specific capture of target proteins by oriented antibodies bound to tyrosinase-immobilized Protein A on a polyallylamine affinity membrane surface, Journal of Membrane Science. 282 (2006) 311–321. doi:10.1016/j.memsci.2006.05.033.
[56] K. Hernandez, R. Fernandez-Lafuente, Control of protein immobilization: Coupling immobilization and site-directed mutagenesis to improve biocatalyst or biosensor performance, Enzyme Microb. Technol. 48 (2011) 107–122. doi:10.1016/j.enzmictec.2010.10.003.
[57] W. Norde, J. Lyklema, The adsorption of human plasma albumin and bovine pancreas ribonuclease at negatively charged polystyrene surfaces. III. Electrophoresis, Journal of Colloid and Interface Science. 66 (1978) 277–284. doi:10.1016/0021-9797(78)90304-1.
[58] Z. Pei, H. Anderson, A. Myrskog, G. Dunér, B. Ingemarsson, T. Aastrup, Optimizing immobilization on two-dimensional carboxyl surface: pH dependence of antibody orientation and antigen binding capacity, Anal. Biochem. 398 (2010) 161–168. doi:10.1016/j.ab.2009.11.038.
[59] J. Lahiri, L. Isaacs, J. Tien, G.M. Whitesides, A strategy for the generation of surfaces presenting ligands for studies of binding based on an active ester as a common reactive intermediate: a surface plasmon resonance study, Anal. Chem. 71 (1999) 777–790. doi:10.1021/ac980959t.
[60] T. Arakawa, Y. Kita, S.N. Timasheff, Protein precipitation and denaturation by dimethyl sulfoxide, Biophysical Chemistry. 131 (2007) 62–70. doi:10.1016/j.bpc.2007.09.004.
[61] S. Bhattacharjya, P. Balaram, Effects of organic solvents on protein structures: observation of a structured helical core in hen egg-white lysozyme in aqueous dimethylsulfoxide, Proteins. 29 (1997) 492–507.
[62] J.M. Bolívar, Latex immunoagglutination assays, Journal of Macromolecular Science Part C - Polymer Reviews. 45 (2005) 59–98. doi:10.1081/MC-200045819.
[63] M.L. Yarmush, K.P. Antonsen, S. Sundaram, D.M. Yarmush, Immunoadsorption: strategies for antigen elution and production of reusable adsorbents, Biotechnol Progr. 8 (1992) 168–178. doi:10.1021/bp00015a001.

755
756

**Captions**

Figure 1. Reaction schemes of the azidification of the silicon slides (A), alkynation of proteins (B), CuAAC immobilization of the proteins (C) and EDC/NHS mediated immobilization of proteins (D).

Figure 2. Native polyacrylamide gel electrophoresis of wild-type SpA (left, three replicate samples) and A-SpA (right, four replicate samples).

Figure 3. Surface mass of four different mixtures in PBS pH 7.4. The dashed line marks the theoretical surface mass of a close-packed monolayer of SpA as estimated by Lahiri et al [59].

Figure 4. Surface mass of four different mixtures dissolved in sodium acetate buffer pH 4. The dashed line marks the theoretical surface mass of a close-packed monolayer of SpA as estimated by Lahiri et al [59].

Figure 5. Surface mass evolution as measured by ellipsometry during consecutive washing steps with acetate buffer (Ac.); washing buffer (WB); sodium dodecyl sulfate solution (SDS); washing buffer and acetate buffer: for A-SpA which is covalently coupled to azidified silicon slides by CuAAC with Mixture 1 in acetate buffer (green) and for control experiments accomplished under identical conditions but with carboxylated plates and/or non-alkynated SpA.

Figure 6. A-SpA Surface Mass evolution of CuAAC coupling using different protein concentrations, followed by subsequent washing steps with WB, SDS and PBS. The insert shows the concentration dependency of the final A-SpA surface mass.

Figure 7. Average Surface Mass (ASM) and standard deviation obtained from immobilizations of SpA on carboxylated silicon slides by physical adsorption and EDC/NHS coupling and of A-SpA on azidified slides with CuAAC.

Figure 8. Average Surface Mass (ASM) of antibody and corresponding standard deviations obtained after binding of human IgG to different SpA functionalized slides.

Figure 9. hIgG Surface Mass evolution after binding to surfaces with different amounts of A-SpA. The binding of hIgG is followed by washing with glycine, SDS and PBS.

Figure 10. Surface mass evolution for the coupling of standard alkynated MBP (green) and fully alkynated MBP (orange) to azidified silicon slides by CuAAC with Mixture 1 and for consecutive washing steps with washing buffer (WB), sodium dodecyl sulfate solution (SDS) and PBS.

Figure 11. Surface mass evolution of the MBP-coupled slides during the binding of monoclonal anti-MBP: standard alkynated A-MBP (green; average increase: 0.13 $\mu$g/cm$^2$) and fully alkynated fA-MBP (orange; average increase: 0.05 $\mu$g/cm$^2$).

Table 1. Reaction mixtures used for the immobilization of SpA in either sodium acetate buffer pH 4 or PBS pH 7.4. All mixtures contain 1$\mu$M of protein.

Table 2. Surface mass measurements and the corresponding standard deviations after 30 min and 18 h of CuAAC reaction. At 30 min a 5 min wash step with WB was performed to see the difference in surface mass.